Electronic SUPPORTING INFORMATION (ESI)

The Nano-Morphological Versatility by Self-Assembly of a Peptide Mimetic Molecule in Response to Physical and Chemical Stimuli

Sudeshna Kar [a], Kung-Wei Wu[a], I-Jui Hsu[b], Chi-Rung Lee [c] and Yian Tai*[a]

[a] *Department of Chemical Engineering, National Taiwan University of Science and Technology, 43 Keelung Road, Taipei-106, Taiwan*

[b] *Department of Molecular Science and Engineering, National Taipei University of Technology Taipei 10608, Taiwan*

[c] *Department of Chemistry and Materials Engineering, Minghsin University of Science and Technology, Hsin-chu 304, Taiwan*

*Corresponding Author:

Prof. Yian Tai

Department of Chemical Engineering, National Taiwan University of Science and Technology, 43 Keelung Road Sec. 4, Taipei 106, Taiwan.

Phone: +886-2-2737-6620, Fax: +886-2-2737-6644

E-mail: ytai@mail.ntust.edu.tw

Experimental Section

(1) Detail synthesis of Boc-*m*ABA-Aib-OMe

Boc-*m*ABA-OH

The amino acid *m*-aminobenzoic acid (6 g, 43.75 mmol) was suspended in a 1:1 tetrahydrofuran (THF) water mixture. Solid $NaHCO_3$ (11.02 g, 131.25 mmol) and Boc-anhydride (10.49 ml, 48.12 mmol) were added to it.The reaction mixture was stirred at room temperature over night. After 24 h, the THF layer should be driven out with the help of vaccum pump. The aqueous layer was cooled in an icebath, acidified with 2M HCl and extracted with ethylacetate. The organic layer was washed with excessof water and dried over anhydrous Na_2SO_4 and evaporated in *vacuo* producing a white solid.

Yield: 9.20 g (88.71%). Anal.Calcd for $C_{12}H_{15}N_1O_4$ (237.247): (C, 60.74; H, 6.37; N, 5.90)%. Found: (C, 60.71; H, 6.39; N, 5.92)%.

Synthesis of the peptide Boc-*m*ABA-Aib-OMe

Boc-*m*ABA-OH (1.25 g, 5.27 mmol) was dissolved in dimethylformamide (DMF; 10 mL). Aib-OMe (1.6 g, 10.54 mmol) obtained from its hydrochloride was added followed by DCC (1.62 g, 7.90 mmol) and HOBT (0.71 g, 5.27 mmol). The reaction mixture was stirred at room temperature for 1 day. The precipitated dicyclohexylurea (DCU) was filtered and diluted with ethyl acetate (80 mL). The organic layer was washed with excess of water, 1M HCl (3 X 30 mL), 1M Na_2CO_3 solution (3 X 30 mL) and again with water. The solvent was then dried over anhydrous Na_2SO_4 and evaporated in *vacuo*, giving a light yellow gum. Purification was done using silica gel as stationary phase and an ethyl acetate-petroleum ether mixture as the eluent.

Single crystals were grown from MeOH by slow evaporation and were stable at room temp. Yield: 1.50 g (84.74%). M.p = 164^0C.

(2) Experiments

NMR Experiments

All ^{1}H NMR and ^{13}C NMR spectra of peptide were recorded on a Bruker Avance 300 model spectrometer operating at 300/500 MHz and 75 MHz respectively. The peptide concentrations were 10 mM in DMSO-D6 for ^{1}H NMR and 40 mM in DMSO-D6 for ^{13}C NMR.

FT-IR Spectroscopy

FT-IR spectra of PMM were examined in Perkin Elmer–782 model spectrophotometer. The solid- state FT-IR measurements were performed using the KBr disk technique.

Mass Spectrometry

Mass spectrum of peptidewas recorded on HEWLETT PACKARD Series 1100MSD and Micromass Qtof Micro YA263 Mass spectrometers by positive mode electro spray ionization.

Field Emission Scanning Electron Microscopic Study

SEM was used to investigate the morphology of the nanostructures. In general, freshly prepared methanolic solutions of peptide (1, 5 and 10 mM) were taken on glass cover slips and evaporated to dryness for 24 h. For solid samples such as vesicles and fibrils formed on different SAMs were directly taken for SEM experiment. A gold coating was applied to the top of the samples to make it conductive for analysis.The micrographs were taken in a FESEM apparatus (JOEL6400).

SEM images were taken at an accelerated voltage of 8 kV. For salt-triggered disruption study 10 mM solutions of KCl salt in methanol-water (1:1 v/v) were added into freshly prepared 10 mM methanolic solution of peptide in 1:1 (v/v) proportion and incubated for 12h, followed by SEM imaging.

Thermal influence under Dry Conditions

The thermal influence on nanostructures was tested by treating dried sample-loaded glass cover slips at a constant temperature of 50, 100 and 150 °C for 1 h and analyzing by SEM. Heat treatment was carried out using a forced air flow programmable convection oven (EYELA, NDO-451SD) having an accuracy of ±1 °C at 250 °C. For thermogravimetric analysis (TGA), a solution of peptides (approximately 3-5.5 mg mL^{-1}) in methanol was aged for 2 days at room temperature and then dried under vacuum. TGA analysis was carried out on a Mettler Toledo TGA/SDTA 851 thermal analyzer in a dynamic atmosphere of dinitrogen (flow rate = 30 cm^3min^{-1}). The sample was heated in an alumina crucible at a rate of 5 °C min^{-1}.

Transmission Electron Microscopic Study

TEM was also carried out to investigate the morphology of the nanostructures. Freshly prepared methanolic solutions of peptide (1 mM, 5 mM and 10 mM) were sonicated with UC 250 W INECO ultrasonicator for 30 min, and one drop of each of these solutions was taken in a carbon-coated copper grid (300 mesh), excess fluid was removed after 1 min and evaporated to dryness under vacuum for 12 h. With these grids, TEM studies were carried out using a Philip Tecnai F20 G2 electron microscope. For solid samples such as vesicles and fibrils formed on different SAMs were directly taken on grids for TEM experiment. TEM images were taken at an accelerated voltage of 200 kV.

Dynamic Light Scattering (DLS) Measurements

Freshly prepared solutions of the peptides (10.0 mM) in methanol-water (9:1 by v/v) were used for dynamic light scattering measurements using a Nano-S-1600, MALVERN, USA instrument, after ultrasonication of the solutions for 30 min.

Fluorescence Study

The encapsulation properties of nanovesicles were examined by the fluorescence study of anticancer drug methotrexate. For this purpose methanolic solution of peptide (1 mM) was incubated with 0.014 mM of methotrexate for 2 d assisted by 30 min ultrasonication. One drop (20 μL) of these solutions was loaded on the glass slide and dried at room temperature under vacuum followed by fluorescence microscopic imaging with an Olympus BX 51 fluorescence microscope at 200× and 400× magnification. Images were captured through cool CCD camera that was attached to the microscope and processed through Image-Pro Express software. For salt-triggered disruption studies, 10 mM 55% methanolic solutions of KCl salt was added to the encapsulated solution of peptide and further incubated overnight followed by fluorescence microscopic imaging (Fluorescence Microscope Olympus BX 61).

UV-Vis analysis

UV-Vis spectrophotometer was used to measure the absorption of peptide and surface Plasmon resonance (SPR) band of gold nano particles.UV absorption spectra (800–200 nm) were recorded with a JASCO V-670 spectrophotometer.

Photoluminence analysis

JASCO FP-6500LE spectroflurometer was used to measure the photoluminence (PL) property of methotrexate. The suitable excitation wavelength was selected at 350 nm.

Single Crystal X-Ray Diffraction

Diffraction data for peptide grown by slow evaporation of methanol was collected with MoKα radiation at 100 K using the Oxford Atlas-CCD diffractometer System. The crystals were positioned 55 mm from the CCD. Frames were measured with a counting time of 50 s. Data analyses were carried out with the CrysAlisPro program. The structures were solved using direct methods with the SHELXL-2013 program (Sheldrick, 2013). The structures were refined on F^2 using SHELXL-2013 (Sheldrick, 2013) to R1=0.039; wR2 =0.103 for 4367 reflections with $I > 2\sigma(I)$. Crystallographic details of peptide have been deposited at the Cambridge Crystallographic Data Centre; reference CCDC no 949965. These data can be obtained free of charge via www.ccdc.cam.ac.uk/conts/retrieving.html (or from the Cambridge Crystallographic Data Centre, 12 Union Road, Cambridge CB21EZ, UK; fax: (+44) 1223-336-033; or e-mail: deposit@ccdc.cam.ac.uk).

Wide Angle X-ray Diffraction (WAXD) Analysis

Wide angle X-ray diffraction (WAXD), a technique for ascertaining the molecular packing of assemblies, was used to investigate the internal structure of the self-assembled nanostructures of PMM. WAXS analysis were performed with wavelength of 1.5406 Å. WAXD patterns of PMM in vesicle form generated from methanol, in fiber form generated on $–CH_3$ SAM, in fiber form generated after thermal treatment at 100 ^{0}C for 1 hr and in fiber morphology generated from ethyl acetate were investigated. The X-ray diffractogram were obtained in the range of 2Θ from

10^{o} to 30^{o}. XRD samples were prepared by dropping PMM solution on the 2cm x 2cm glass substrate. The 2θ/ω-scan XRD patterns were carried out on a PANalytical X'Pert PRO MRD system with offset ω-angle of +0.5º.

(3) Detail characterization of Boc-*m*ABA-Aib-OMe

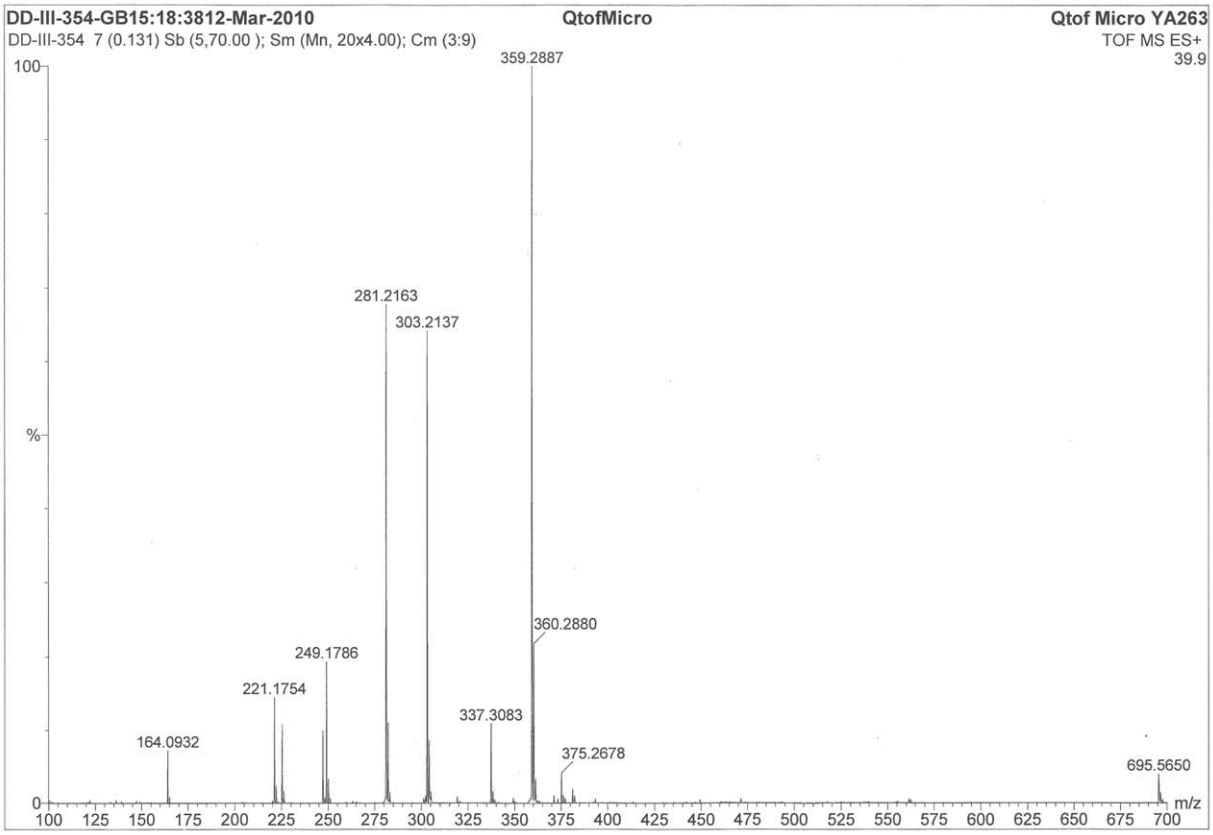

Mass spectrum of peptide

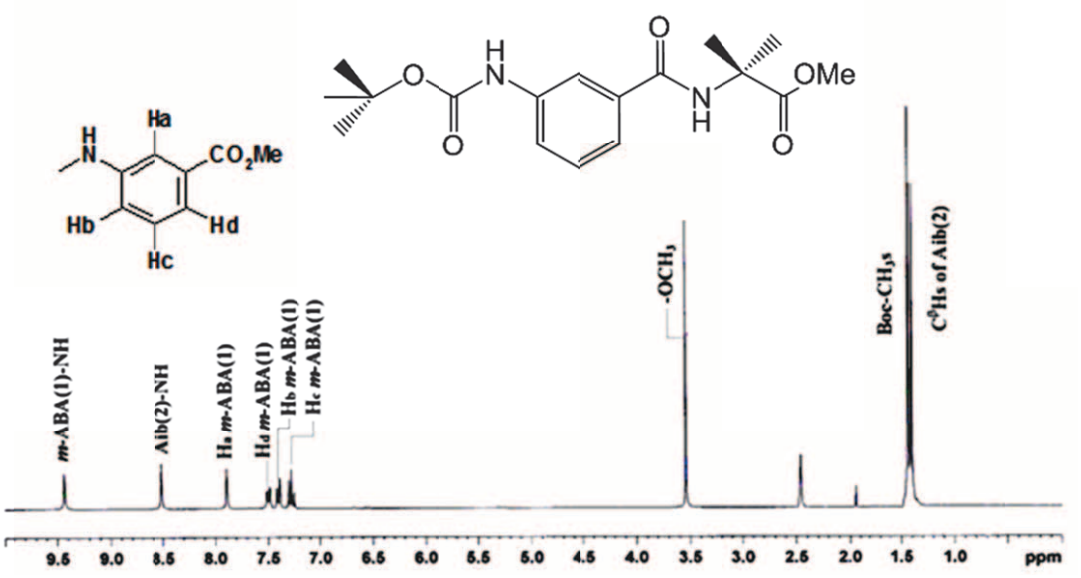

^{1}H NMR spectrum of peptide in DMSO-D6 (300 MHz)

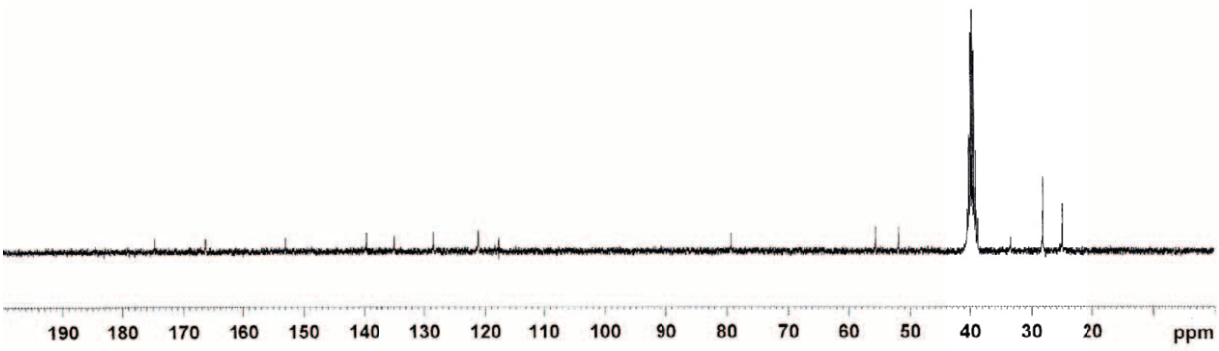

^{13}C NMR spectrum of peptide in DMSO-D6 (75MHz)

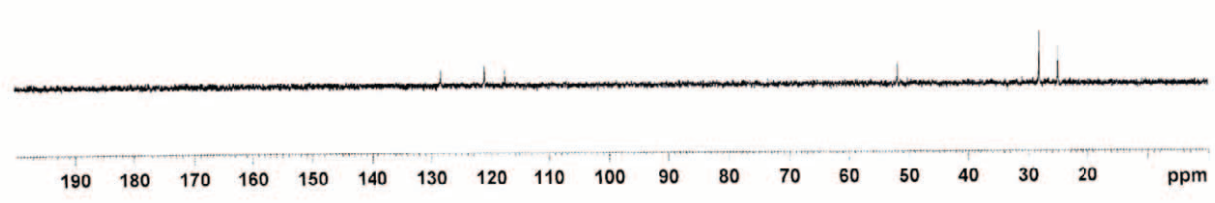

DEPT-135 spectrum of peptidein DMSO-D6 (75MHz)

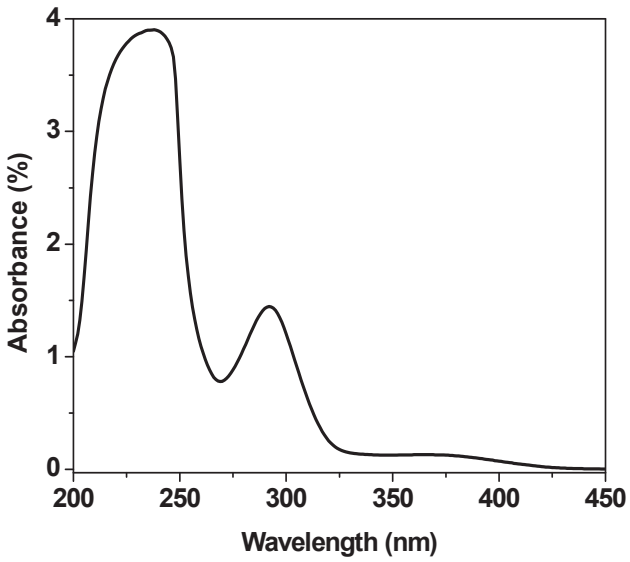

UV spectrum of 1 mM methanolic solution of peptide

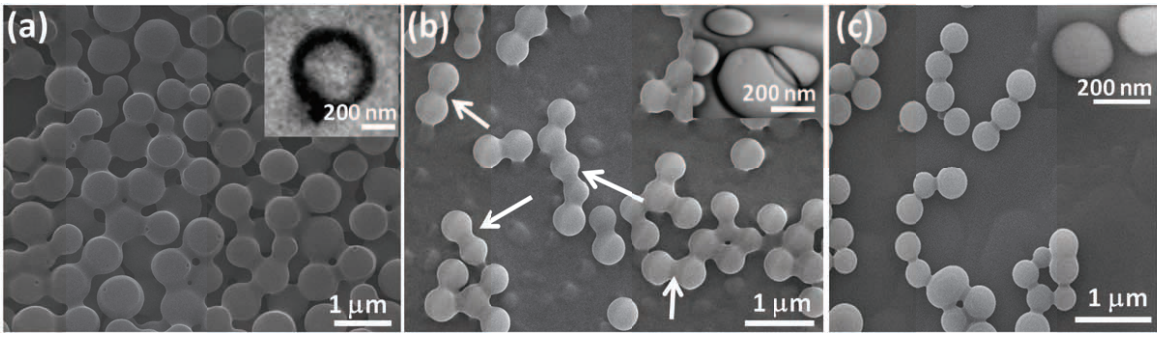

Fig. *S1* FE-SEM images of methanolic solutions of peptide at concentrations of: (a) 10 mM; (b) 5 mM, arrows indicate the fused spherical structures and (c) 1 mM solutions. In the insets of (a), (b) and (c) the TEM images show the hollow nature of the spherical structures

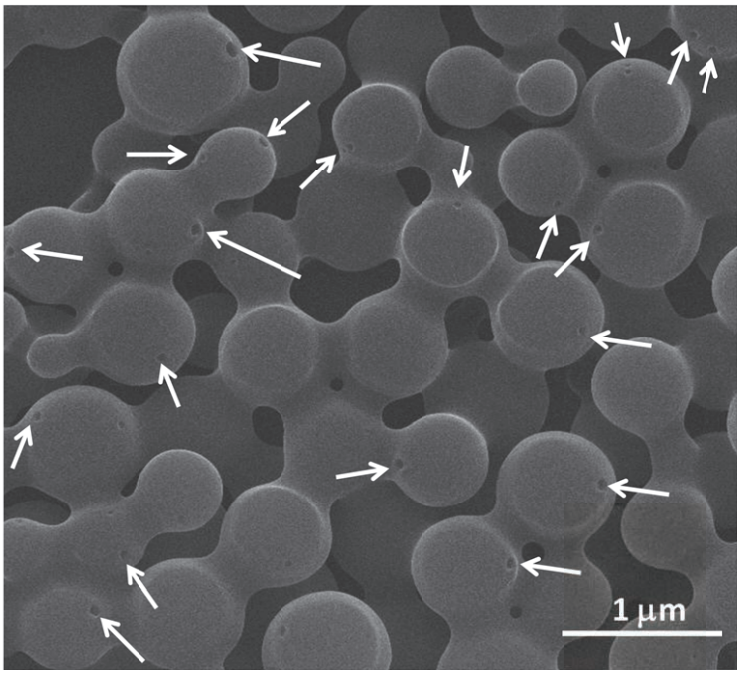

Fig. *S2* Enlarged FE-SEM image of PMM spherical structures generated from methanolic solutions having concentration of 10 mM, arrows indicate the holes on the vesicles, which establish the porous nature of the PMM spherical structures

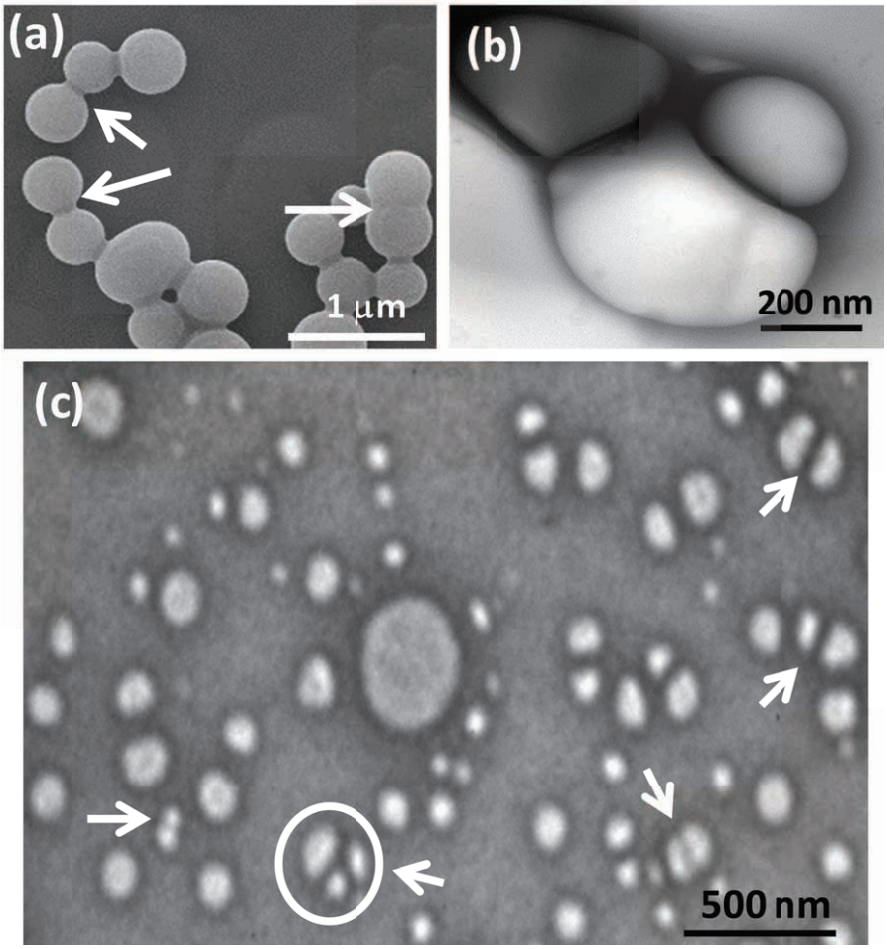

Fig. *S3* (a) FE-SEM images of methanolic solutions of peptide, arrows indicate the fused vesicles; (b) TEM image of fused vesicles; and (c) TEM image showing the hollow nature of the vesicles and the arrows and encircled portion indicate the fused vesicles

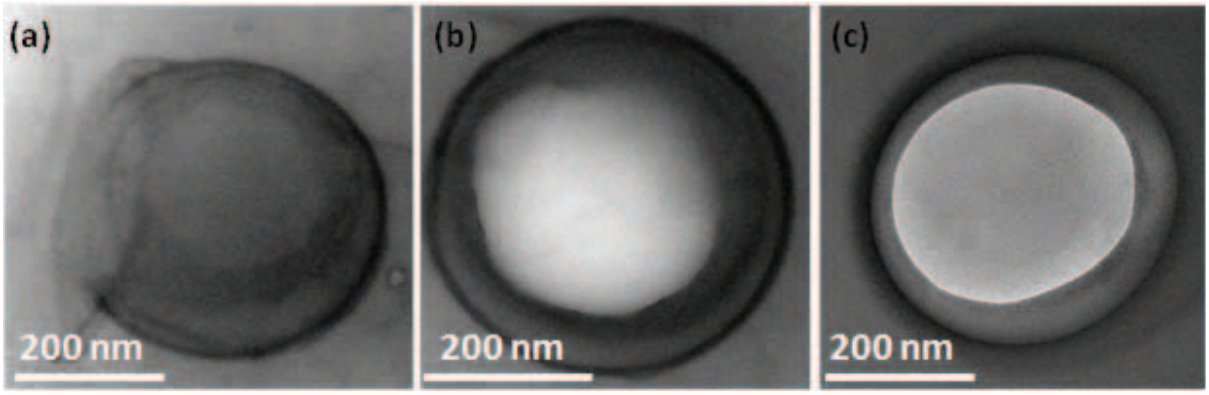

Fig. *S4* TEM images showing stepwise damage of outer film of a vesicle generated from 10 mM methanolic solution of **Boc-*m*-ABA-Aib-OMe** by electron beam to prove the hollow nature of it. (a) TEM image of vesicle having intact outer film; (b) TEM image of vesicle having partly damaged outer layer by electron beam irradiated on it for 5 seconds; and (c) TEM image showing vesicle with hollow cavity inside of it after irradiation by electron beam for 10 seconds

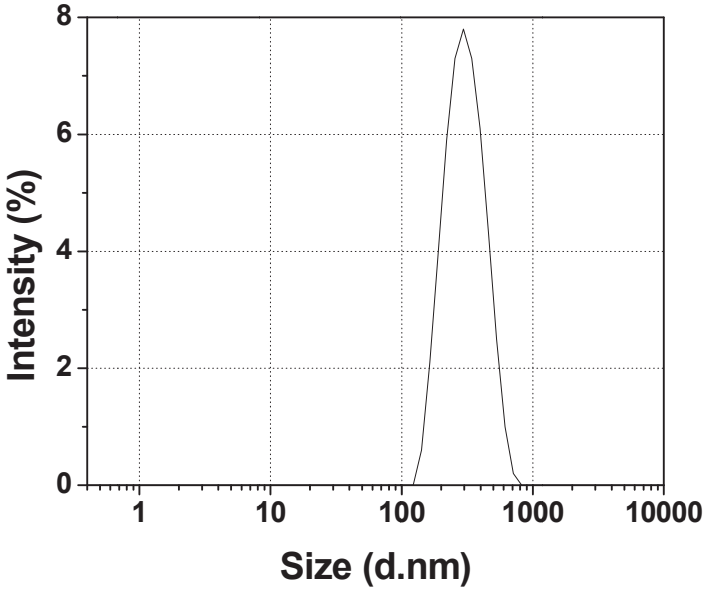

Fig. *S5* Size distribution profile in DLS study, peptide showing hydrodynamic diameter, 320.25 nm and polydispersity index, 0.30.

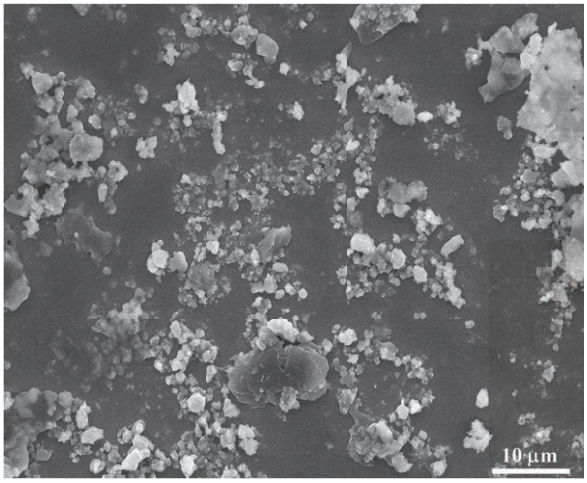

Fig. *S6* FE-SEM images of peptide, showing unstructured morphology in the solid state, when heated above 150 °C.

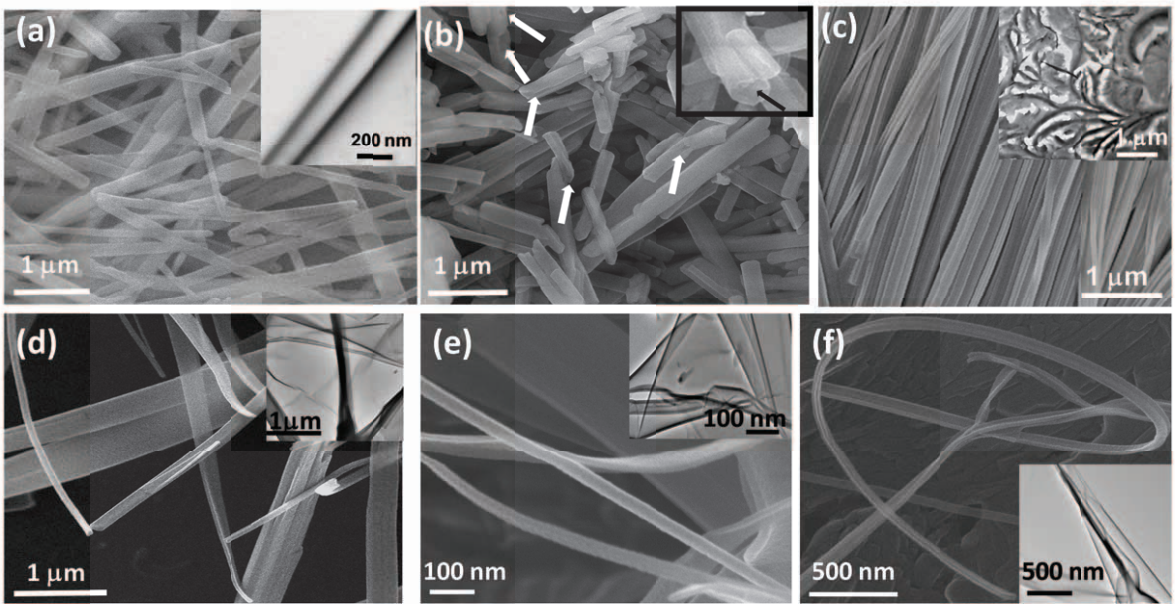

Fig. *S7* FE-SEM images of peptide, showing formation of nano-tubes, when grown from (a) $CHCl_3$-MeOH mixture (1:1 v/v) and (b) toluene; in (a), the inset shows the TEM image of hollow tube; in (b) the hollow nature has been pointed with arrows and an enlarged image of hollow tube has been shown in the inset; the FE-SEM image in (c) shows the formation of nano-fibrils from ethyl acetate solvent; the FE-SEM images in (d)-(f) show the formation of flat tape or ribbon like structure while grown from $CHCl_3$-Petroleum ether mixture (1:1 v/v), acetone and DMF solution respectively; Concentration of peptide was maintained at 10 mM in all the solvents. Insets in (d)-(f) show the TEM images of the nano-fibrils

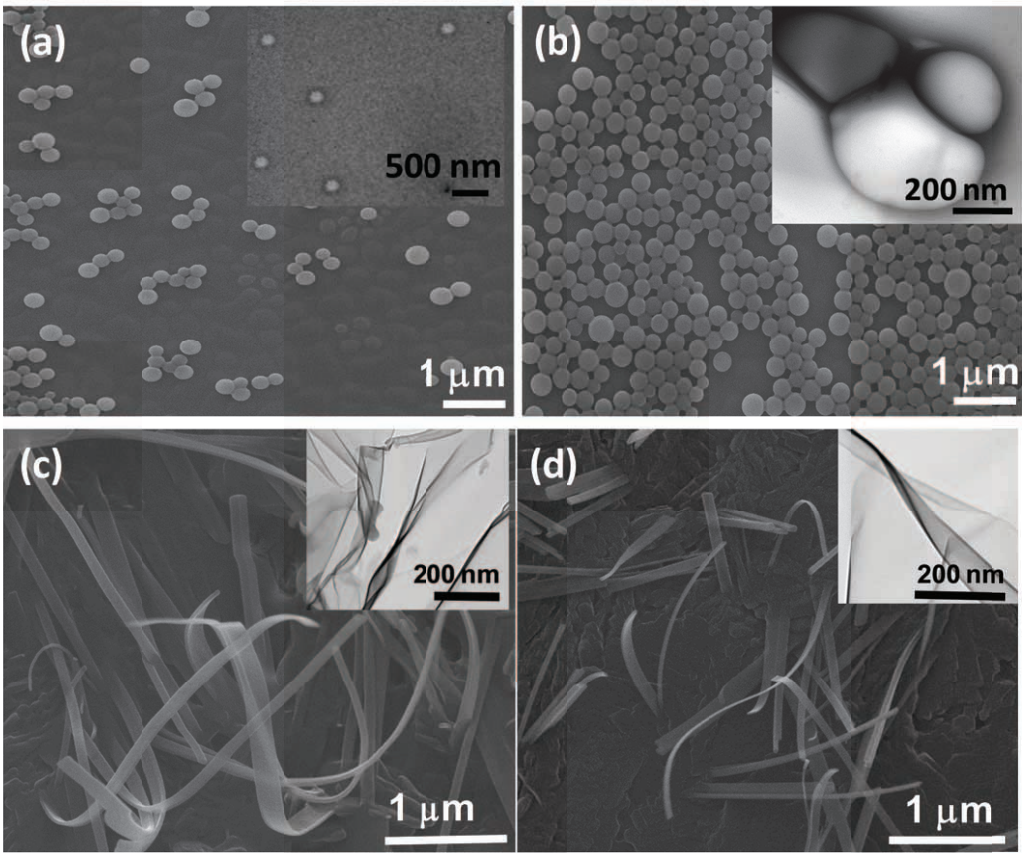

Fig. *S8* FE-SEM images show the formations of vesicles from methanolic solution of peptide generated on (a) -NH_2 SAM and (b) -SH SAM surfaces, respectively; in the insets of (a) and (b) the TEM images show the hollow nature of the vesicles; FE-SEM images show the formations of nano-ribbons/fibrils on (c) -CH_3 SAM and (d) -C8 SAM surfaces respectively. TEM images in the inset of (c) and (d) clearly depict the nature of nano-ribbon/fibrils

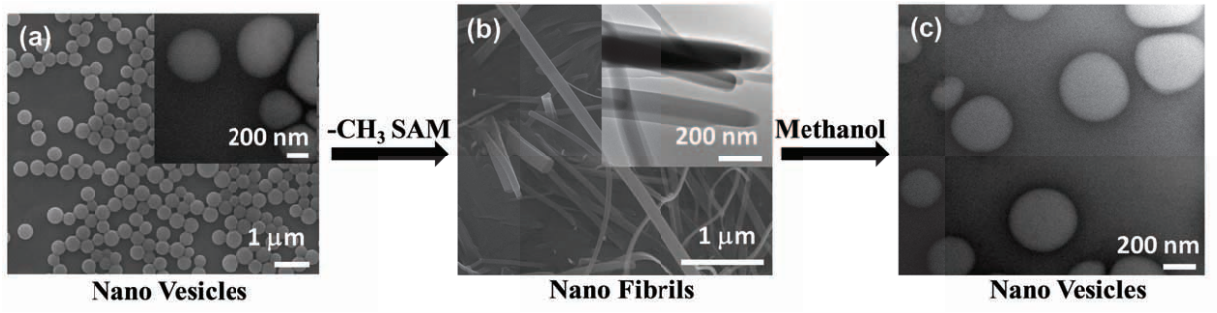

Fig. *S9* (a) FE-SEM images show the formations of vesicles from methanolic solution of PMM generated on glass surface; in the insets of (a) TEM image show the hollow nature of the vesicles; (b) FE-SEM images show the formations of nano-ribbons/fibrils on -CH_3 SAM. TEM image in the inset of (b) clearly depict the nature of nano-ribbon/fibrils; (c) TEM image of nano-vesicles generated from the PMM fibrils on -CH_3 SAM, when they were treated with methanol.

Table *S1* Solid state FT-IR spectral analysis of as synthesized peptide and its vesicular form

	N–H stretching vibration &overtone of the N–H bending vibration (cm^{-1})	C=O stretching vibration in ester group (cm^{-1})	C=O stretching vibrations of the peptide urethane,amide I, and bending peaks of amide II (cm^{-1})
As-synthesized peptide	3347.43, 3251.31-3271.07(Shoulder band)	1745.73	1704.37,1644.56, 1592.70, 1558.43, 1535.67
Vesicle formation from methanol solvent	3348.36, 3251.65-3271.6(Shoulder band)	1745.56	1706.16, 1644.85, 1592.92, 1558.42, 1534.88
Tube formation from toluene solvent	3347.35, 3270.46 (broad peak)	1745.68	1704.05, 1643.92, 1592.81, 1555.78, 1534.54
Fiber formation on $–CH_3$ SAM	3346. 45, 3269.76 (broad peak)	1745.29	1703.14, 1644.27, 1592.57, 1558.55, 1534.49
Nano-tape/ribbons formation from acetone solvent	3346.91, 3249.75-3275.46(Shoulder band)	1745.56	1705.30, 1644.44, 1591.57, 1558.23, 1535.51

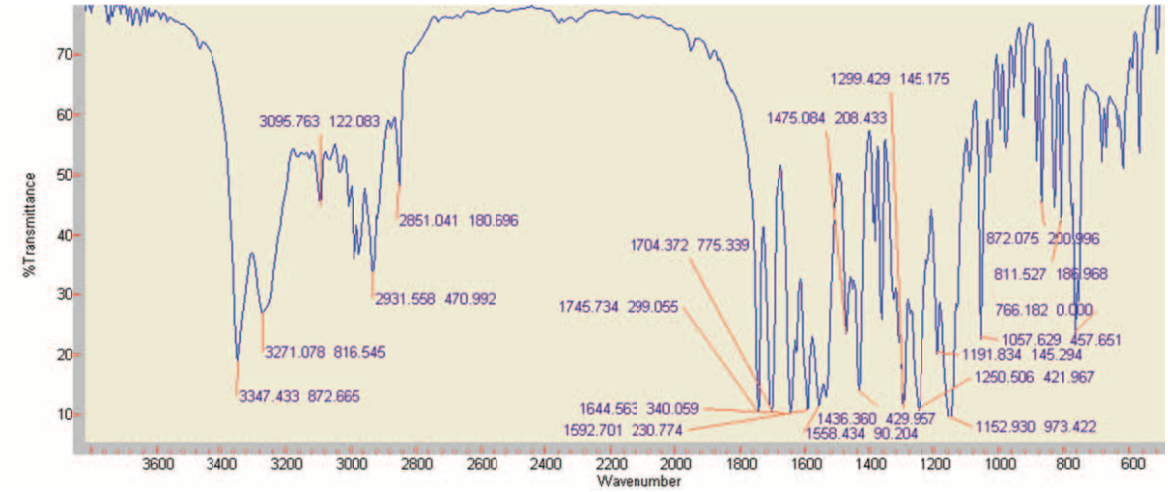

IR spectrum of as-synthesized peptide

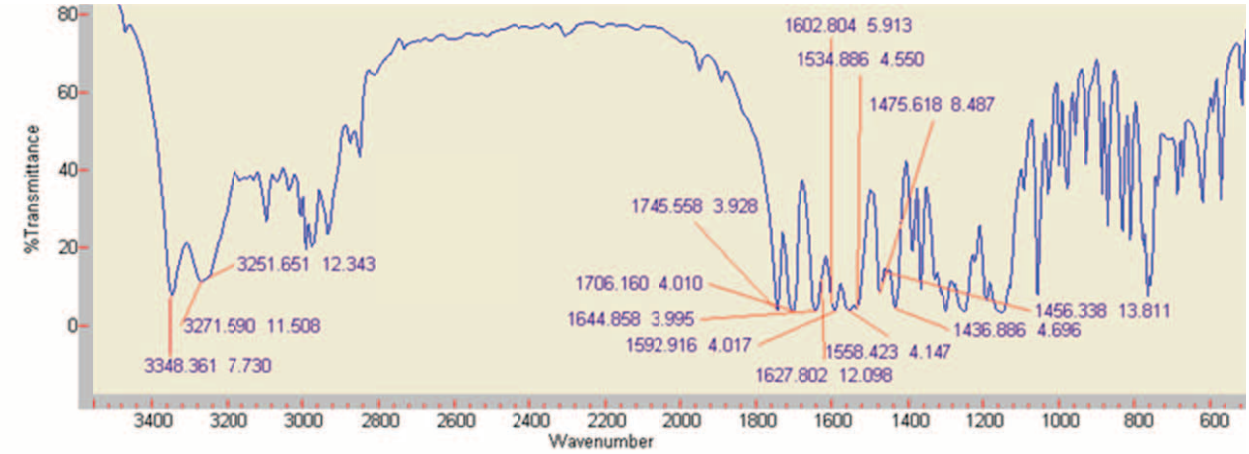

IR spectrum of peptide nano-vesicles generated from methanol

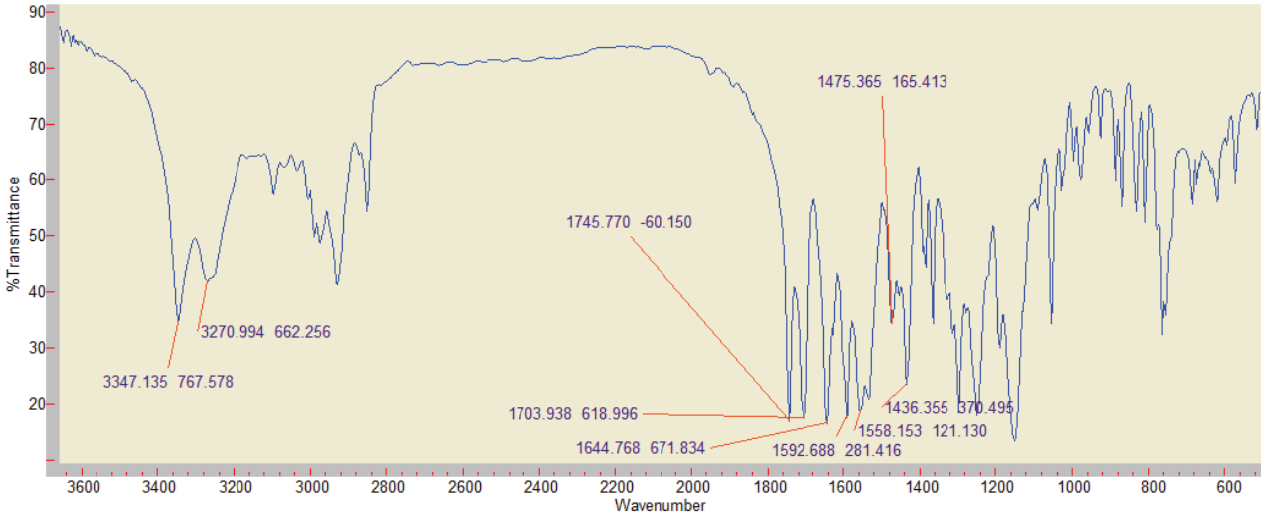

IR spectrum of peptide nano-fibrils generated after thermal treatment at 50 ^{0}C for 1 hr

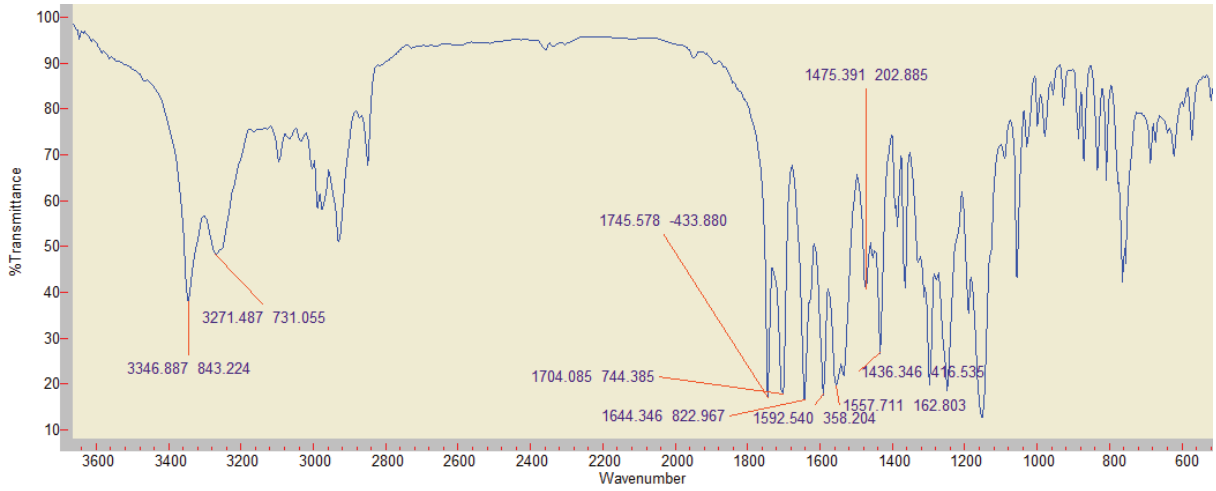

IR spectrum of peptide nano-fibrils generated after thermal treatment at 100 ^{0}C for 1 hr

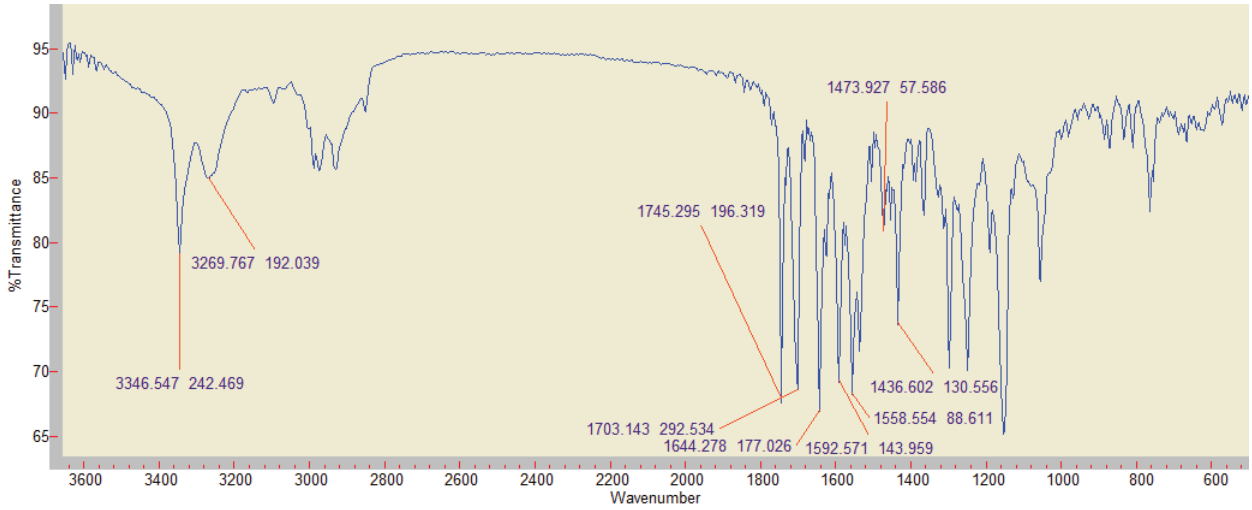

IR spectrum of peptide nano-fibrils generated on –CH_3 SAM surface

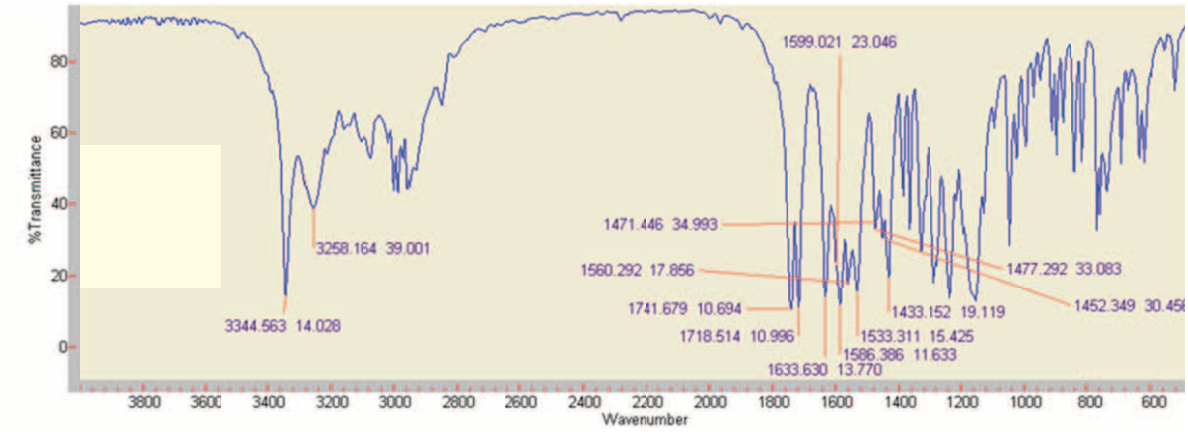

IR spectrum of peptide nano-fibrils generated from ethyl acetate solvent

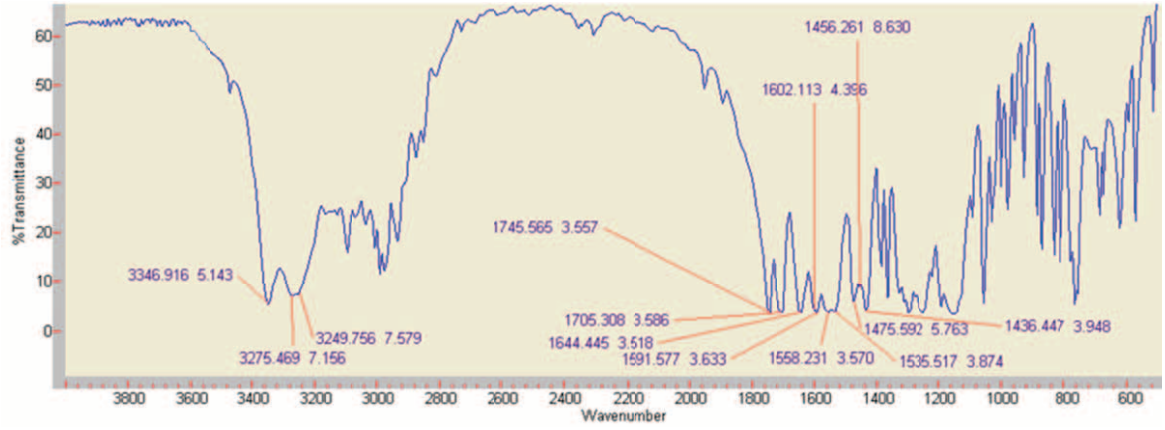

IR spectrum of peptide nano-tape/ribbons generated from Acetone

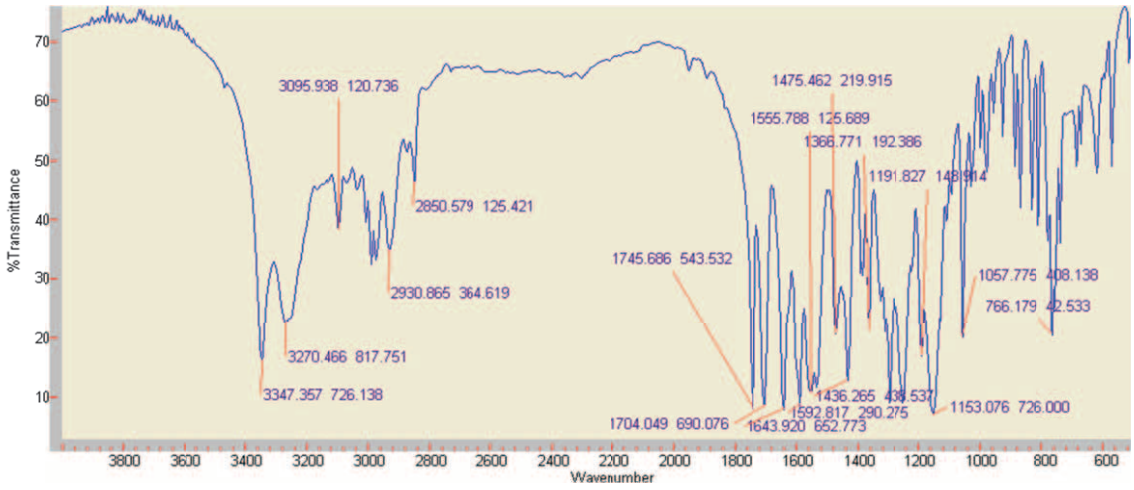

IR spectrum of peptide nano-tubular structures generated from toluene

Fig. *S10* IR spectra of peptide having different morphologies in solid state

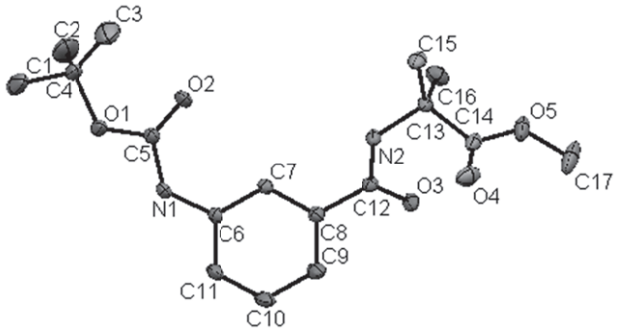

Fig. *S11* ORTEP diagram of PMM backbone.

Table *S2* Selected backbone torsion angles (°) for PMM

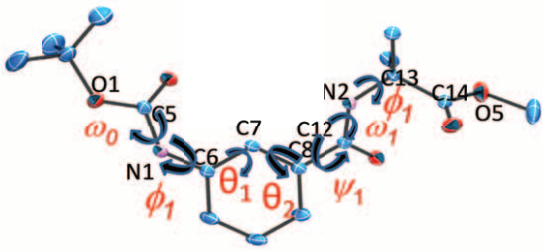

N1-C5-O1-C4	-179.36	N2-C12-C8-C7 (ψ_1)	22.86
C6-N1-C5-O1 (w_0)	-177.33	C13-N2-C12-C8 (w_1)	-178.95
C7-C6-N1-C5(ϕ_1)	24.44	C14-C13-N2-C12 (ϕ_2)	-55.76
C8-C7-C6-N1 (θ_1)	177.22	O5-C14-C13-N2 (ψ_2)	145.57
C12-C8-C7-C6 (θ_2)	177.74		

Table *S3* Intermolecular hydrogen bonds parameters for PMM

Type	N....O/(Å)	H....O/(Å)	O....H-N/(°)
N(2)-H(2)...O(2)[a]	2.943	2.078	176.19
N(1)-H(1)...O(3)[b]	2.934	2.102	159.94

Symmetry elements: [a] -x, y, -z+1/2; [b] -x+1/2, y-1/2, -z+1/2

Table *S4* Crystallographic refinement details for PMM

Crystallographic refinement details	**Peptide**
Crystal Colour	Colourless
Chemical Formula	$C_{17}H_{24}N_2O_5$
Formula Weight (g)	336.37
Crystal System	monoclinic
Space group	C 2/c
Z	8
a (Å)	14.2575(5)
b (Å)	13.1713(4)
c (Å)	20.8636(8)
α(°)	90.00
β (°)	108.856(4)
γ(°)	90.00
V (Å^3)	3707.7(2)
density (gcm^{-3})	1.205
Temperature (K)	100.1(1)
Unique reflections	4847
reflections I>2σ(I)	4367
Nº Parameters	226
GoF	1.039
R_1 [I>2σ(I)], all	0.039, 0.043
wR_2[I>2σ(I)], all	0.103, 0.106
residual electron density (e/Å^3)	0.434, -0.244

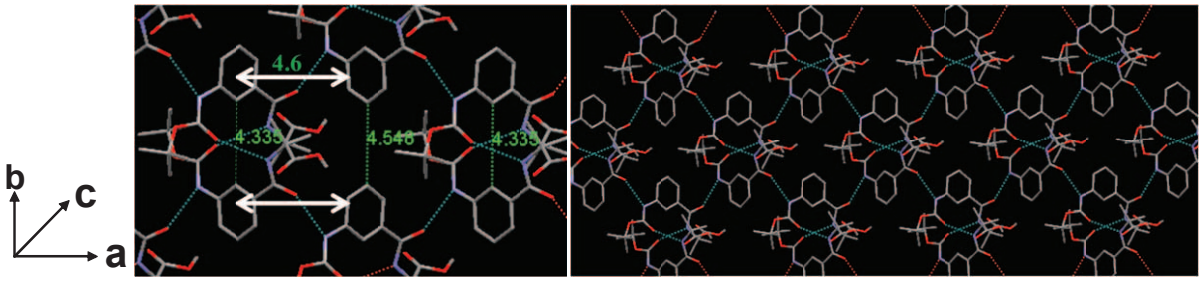

Closest distance between two aromatic rings = 4.33, 4.5 & 4.6 A^0

β-sheet like structure in *ab* plane

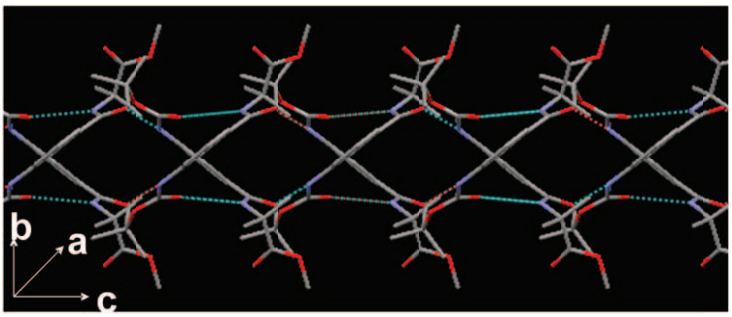

View of the β-sheet layer from *a*-direction

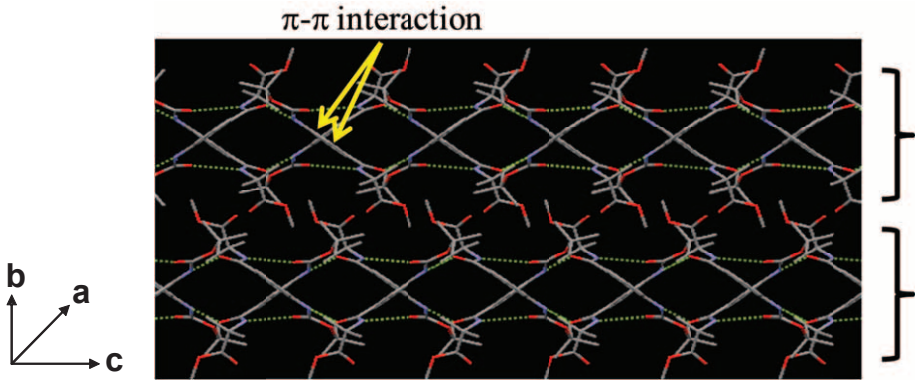

Two β-sheet layers are held by non-covalent interactions

Fig. *S12* Single crystal X-ray diffraction study of PMM. Supramolecular β-sheet-like structure in the *ab* plane of the PMM. Higher order self-assembly of the β-sheet layers in the *b*-direction.Hydrogen atoms are not shown for clarity

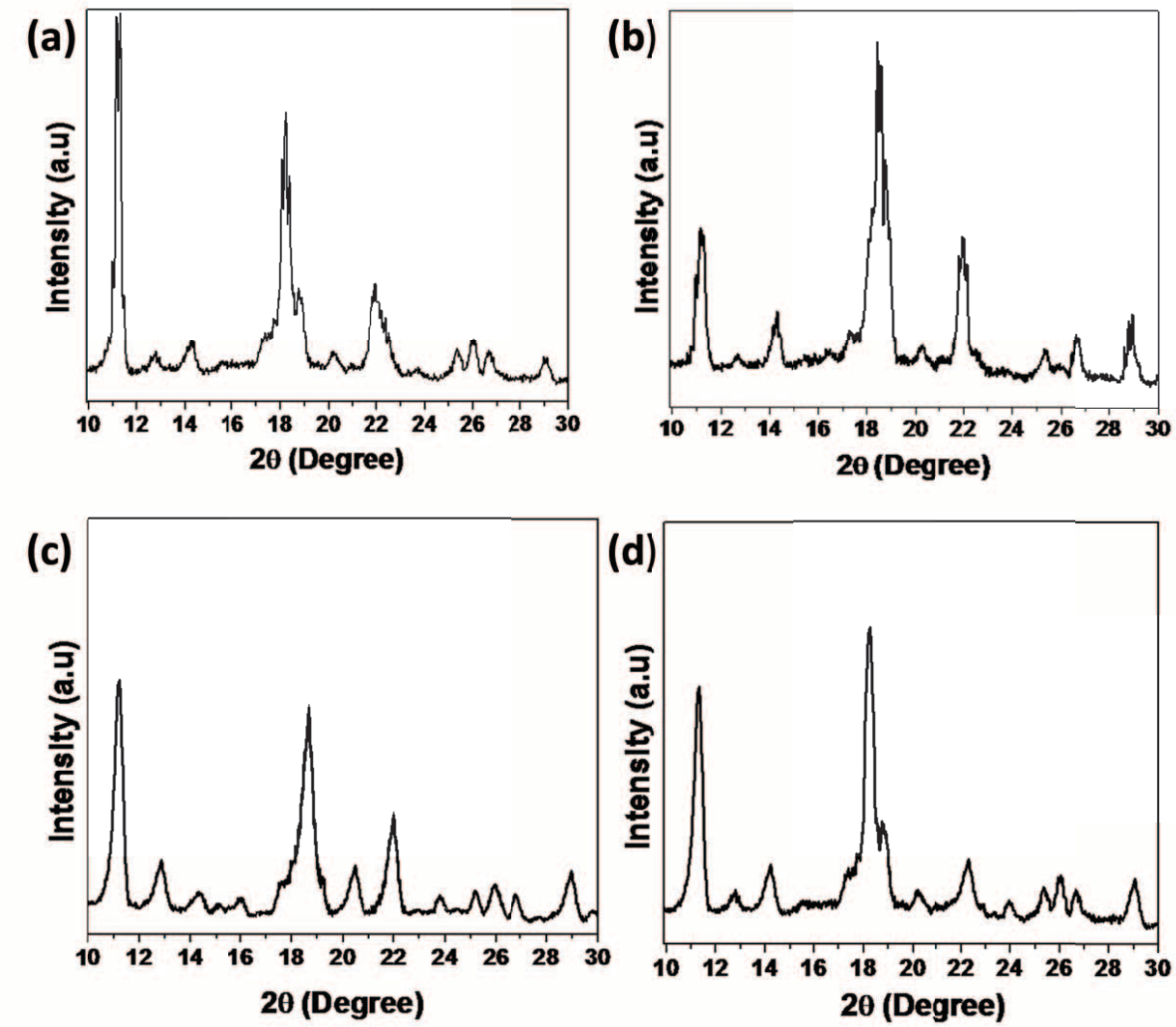

Fig. ***S13*** Wide angle X-ray diffraction (WAXD), a technique for ascertaining the molecular packing of assemblies, was used to investigate the internal structure of the self-assembled nanostructures; WAXS analysis were performed with wavelength of 1.5406 Å. WAXD patterns of PMM (a) in vesicle form generated from methanol, (b) in fiber form generated on $-CH_3$ SAM, (b) in fiber form generated after thermal treatment at 100 ^{0}C for 1 hr and (d) in fiber morphology generated from ethyl acetate; It is clear that the diffraction peaks are at similar position; therefore it can be concluded that both the vesicles and the fibers are generated by similar kind of higher order self-assembly

Table *S5*. Wide angle X-ray diffraction (WAXD) analysis of PMM in different morphologies

Vesicles		***Fibers generated on - CH_3 SAM***		***Fibers generated at 100 ^{0}C***		***Fibers generated from Ethyl acetate***	
2θ	*d-spacing (A˚)*	*2θ*	*d-spacing (A˚)*	*2θ*	*d-spacing (A˚)*	*2θ*	*d-spacing (A˚)*
11. 27	7.84	11.28	7.83	11. 32	7.83	11. 32	7.83
12.81	6.90	12.77	6.92	12.82	6.91	12.79	6.92
14.36	6.16	14.39	6.15	14.38	6.15	14.37	6.15
18.29	4.84	18.29	4.85	18.26	4.84	18.27	4.84
20.22	4.38	20.32	4.36	20.30	4.38	20.23	4.37
22.11	4.01	22.07	4.02	22.10	4.02	22.12	4.02
25.38	3.50	25.37	3.50	25.39	3.50	25.38	3.50
26.02	3.42	25.98	3.42	26.01	3.42	26.02	3.42
26.08	3.40	26.65	3.34	26.06	3.39	26.07	3.38
29.12	3.06	29.10	3.06	29.11	3.06	29.11	3.06

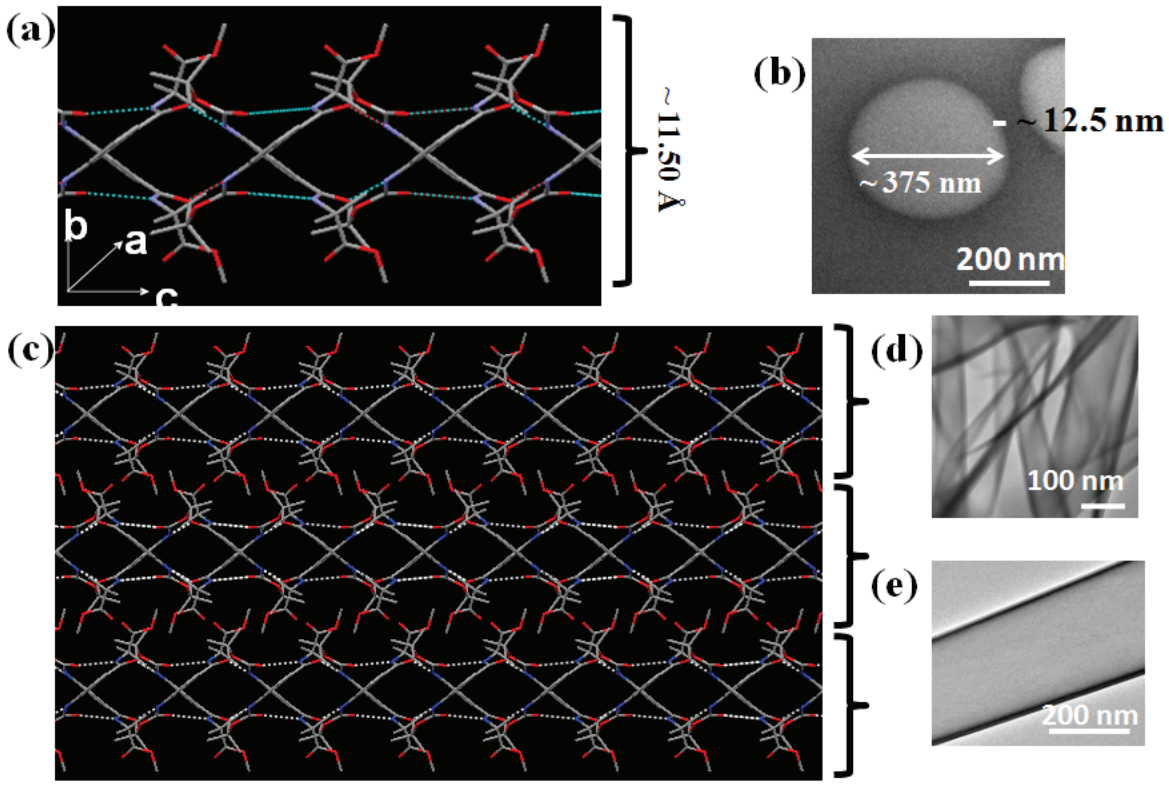

Fig. *S14* A simple co-relation with the crystal structure and the TEM image of PMM nano-structures. In (a) view of the β-sheet like layer from *a*-direction is shown; approximate width of each layer has been calculated as ~ 11.5 Å. In (b) TEM image of one vesicle has been shown; the width of outer layer was calculated as ~ 12.5 nm and hollow space inside was found to be ~375 nm. (c) Higher order self-assembly of the β-sheet like layers in the *b*-direction. Hydrogen atoms are not shown for clarity. Therefore it is assumed that the outer surface of PMM vesicle is constituted of many β-sheet like layers just as shown in (c); though in (c) only 3 such layers are shown for clarity. (d) and (e) are the TEM images of PMM nano-fiber and nano-tube; analyzing the nano structures and the self-assembly of PMM β-sheet like layers, it is predicted that the fibers and the outer layer of tubes are also made up of multilayered stacking of β-sheet like layers of PMM, just like the outer layer of a PMM vesicle

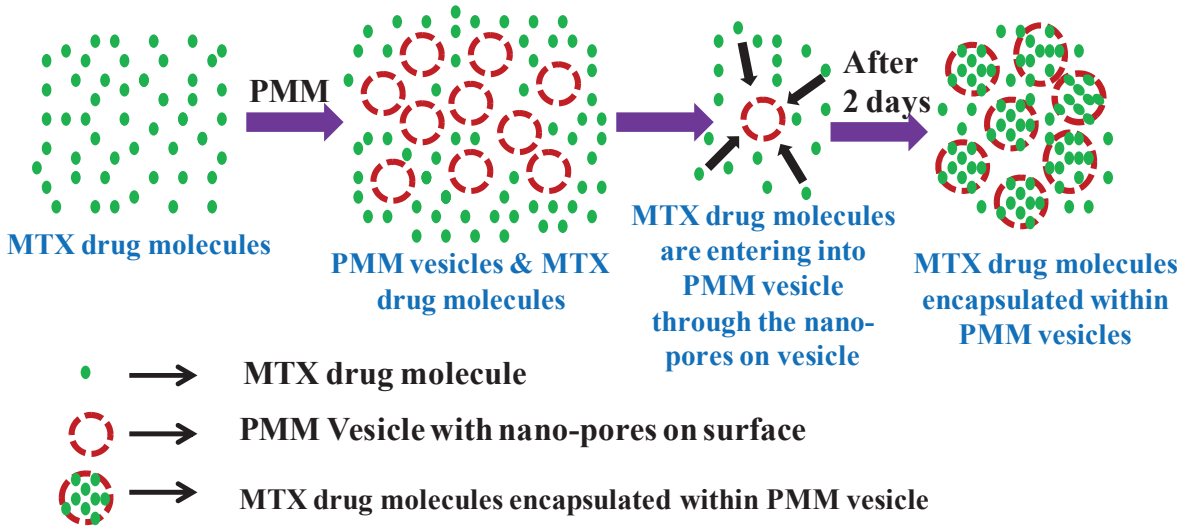

Fig. *S15* Probable mechanism of MTX drug encapsulation by the PMM vesicles

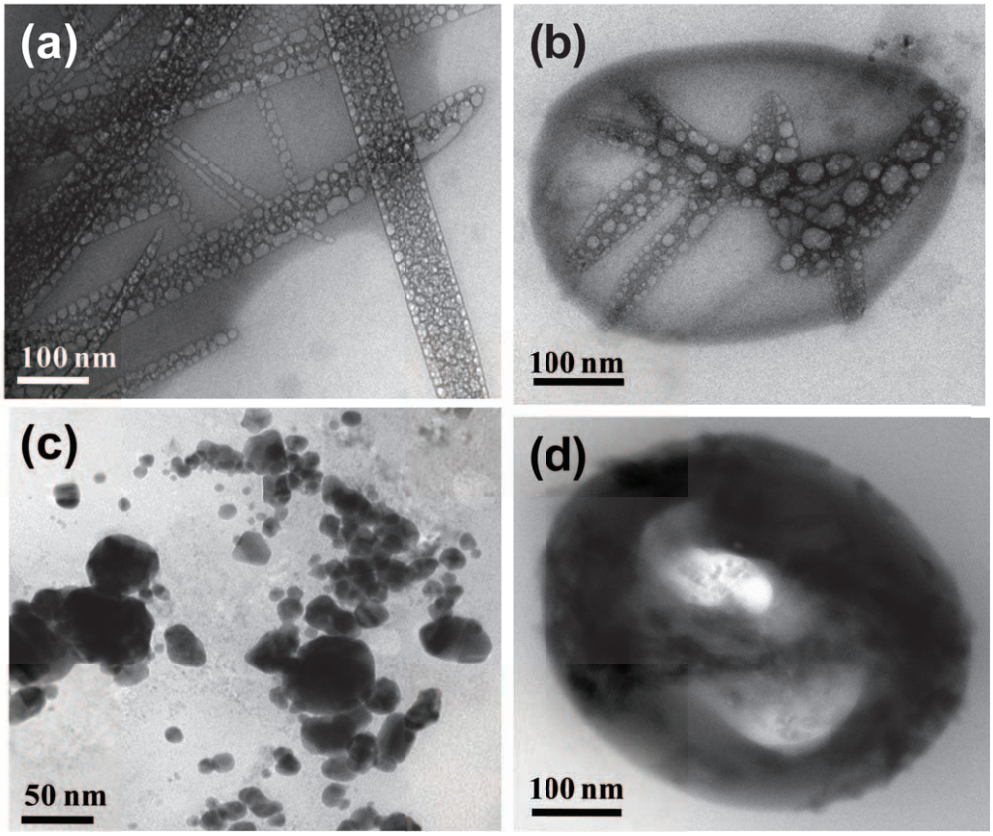

Fig. *S16* TEM images of (a) 7 days aged 0.014 mM methotrexate solution; (b) methotrexate loaded PMM vesicle after 7 days incubation; (c) 2 months aged 0.014 mM methotrexate solution and (d) methotrexate loaded PMM-vesicle of after 2 months